Electronic spectra of oxygen containing polycyclic hydrocarbon cations and the protonated analogues

Arghya Chakraborty, Jan Fulara, and John P. Maier'

Electronic spectra of oxygen containing polycyclic hydrocarbon cations and the protonated analogues

Arghya Chakraborty,[1] Jan Fulara,[1,2] and John P. Maier[1,a)]

[1]*Department of Chemistry, University of Basel, Klingelbergstrasse 80, CH-4056 Basel, Switzerland*
[2]*Institute of Physics, Polish Academy of Sciences, Al. Lotników 32/46, PL-02-668 Warsaw, Poland*

The electronic transitions of 9-fluorenone **FL**$^+$ and 2,3,6,7-dibenzotropone **DBT**$^+$ cations were detected in 6 K neon matrices following a mass-selective deposition. The absorptions at 649.2 and 472.2 nm are assigned to the 2 $^2B_1 \leftarrow \tilde{X}$ $^2A_2$ **FL**$^+$ and 2 $^2A' \leftarrow \tilde{X}$ $^2A'$ **DBT**$^+$ transitions. Absorption spectra of protonated 9-fluorenone **H**$^+$-**FL** and 2,3,6,7-dibenzotropone **H**$^+$-**DBT** have also been measured. Protonation of the oxygenated polycyclic aromatic hydrocarbons is carried out in a hot cathode source via *in situ* produced protonated ethanol. Vibrationally resolved absorptions commencing at 423.3 nm of **H-FL**$^+$ and two band systems of **H-DBT**$^+$ with origins at 502.4 and 371.5 nm are assigned to the 2 $^1A' \leftarrow \tilde{X}$ $^1A'$ electronic transition of 9-hydroxy-fluorenyl cation and 1 $^1A \leftarrow \tilde{X}$ ^1A, 2 $^1A \leftarrow \tilde{X}$ ^1A of 2,3,6,7-dibenzocycloheptenol cation. The assignments are based on vertical excitation energy calculations with time dependent density functional theory, symmetry adapted cluster configuration interaction, and MS-CASPT2 methods. © *2015 AIP Publishing LLC.* [http://dx.doi.org/10.1063/1.4929484]

I. INTRODUCTION

A significant portion of carbon in interstellar medium is supposed to be in the form of polycyclic aromatic hydrocarbons (PAHs). The broad infrared emission features detected from various astronomical environments, the unidentified infrared emission bands (UIR), are often assigned to vibrational transitions of PAHs and their ions.[1–6] In dense molecular clouds or disks of young stellar objects where temperatures are low 10-20 K, PAHs are believed to be condensed on interstellar grains as part of molecular ices, containing mainly water. It is expected that the grain surface could be an important site for prebiotic chemistry. Therefore, laboratory exploration of PAHs on cosmic ice analogs upon ultra-violet radiation became a topic in astrochemistry, and several experiments were carried out by varying the temperature, size of aromatics, and using ice of different molecules (e.g., H_2O, O_2, CO_2, HCN, NH_3).[7–12] The results demonstrate that ices modify the organics and even create new systems during radiation. In the case of H_2O mantels, formation of ketones and alcohols of the corresponding PAHs is predominant.[8,10]

As closed shell PAHs generally have the strongest absorption more to the UV region, their radical cations (PAH$^+$s) and isoelectronic protonated analogues (H-PAH$^+$s) became a subject for spectroscopy and quantum chemistry.[13] These experimental and theoretical studies revealed that most of the H-PAH$^+$s and PAH$^+$s have their strongest absorption in the visible, which may be relevant as possible diffuse interstellar band (DIB) carriers. However, recently measured gas-phase spectra of protonated pyrene and coronene do not correspond to any DIBs.[14,15] In this context, oxygenated analogs of PAHs have not been much studied except for few photoelectron spectra.[16] Oxygen containing PAHs (O-PAHs) could be present

in astronomical environments as incorporation of oxygen is apparent from the UV photolysis of PAHs in solid H_2O.[8] Aromatic ketones have been reported in meteorites[17,18] and solid state ^1H and ^{13}C NMR measurement on meteoritic organic matter reveals the presence of aromatic species along with oxidized sp^2 carbon.[19]

In addition to the possible astrophysical importance, O-PAHs are also detected in the soot of woods and organic oils.[20,21] The percentage of oxygen containing species is dependent on the airflow and temperature.[22] Oxygen atoms can be incorporated in reactions with molecular oxygen or *in situ* from carbon oxides. Hence, the spectroscopic characterization of the O-PAH class of species is of interest for their formation mechanism during terrestrial combustion processes.

In this paper the electronic absorption spectra of two O-PAHs, 9-fluorenone **FL**$^+$, and 2,3,6,7-dibenzotropone **DBT**$^+$ cations and their corresponding protonated species **H-FL**$^+$ and **H-DBT**$^+$ are reported. Electronic spectra were recorded after mass selected deposition of ions in 6 K neon matrices. The assignment of the transitions is made on the basis of calculated excitation energies with the symmetry adapted cluster configuration interaction (SAC-CI), time dependent density functional theory (TD DFT), MS-CASPT2 methods.

II. EXPERIMENTAL

The proton transfer technique is an energetically soft approach applied in mass spectrometry. The solid precursor, 9-fluorenone **FL**, or 2,3,6,7-dibenzotropone **DBT**, was heated in an oven and carried to the source by ethanol EtOH vapor which served as the protonating agent. The structures of the precursors are shown in Chart 1. The protonated O-PAHs are produced in the source *in situ* via protonated ethanol EtOH$_2^+$. It has been previously demonstrated that high pressure of EtOH vapor in the source favors the formation of EtOH$_2^+$ and as a

a)Author to whom correspondence should be addressed. Electronic mail: j.p.maier@unibas.ch. Tel.: +41 612673826. Fax: +41 612673855.

9-fluorenone (FL)
m/z=180

2,3,6,7-dibenzotropone (DBT)
m/z=206

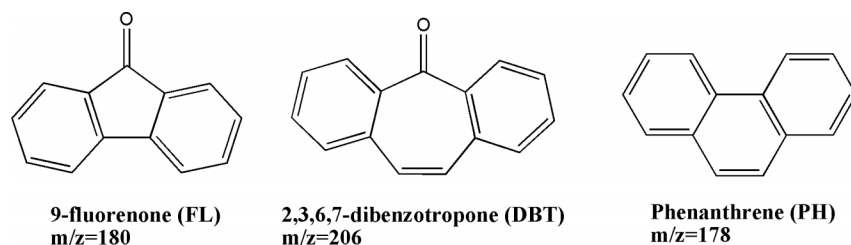**Phenanthrene (PH)**
m/z=178

CHART 1. Structure of the precursor molecules.

consequence the production of protonated PAH.[23] In vapor of pure O-PAHs, the molecular ion M^+ had the highest intensity in the mass spectrum while the $M^+ + 1$ signal grew with EtOH presence (Figure 1). The ions produced were extracted by electrostatic lenses, deflected by 90° to separate cations from neutrals, and guided into a quadrupole mass-filter. The mass-selected ions (1 amu resolution) were co-deposited with excess of neon atoms on the surface of a rhodium coated sapphire substrate held at 6 K. The host neon was contaminated by CH_3Cl in a ratio 30 000:1 to improve the trapping of cations. Free electrons become available in the matrix by the impingement of ions on metal walls near the substrate. These are captured by the CH_3Cl scavenger followed by dissociation into $CH_3^{\bullet}$ and Cl^-. Presence of Cl^- favors the deposition of cations by decreasing the space charge during matrix growth. The $CH_3^{\bullet}$ and Cl^- fragments do not absorb in the experimental detection range; the range for spectral measurement is 250-1100 nm. Electronic spectra are recorded normally after accumulation of at least 10-15 μC of ions in matrix. The absorptions were measured by a "wave-guide" technique.[24] Broad band light from two sources, halogen or a high pressure xenon lamp, was passed through the 20 mm path length of the matrix, then collected by optical fibers, wavelength dispersed by a spectrograph and recorded by the CCD cameras.

III. COMPUTATION

9–fluorenone **FL** and 2,3,6,7-dibenzotropone **DBT** have five and six non-equivalent protonation sites, respectively. Computational data are needed for the determination of the
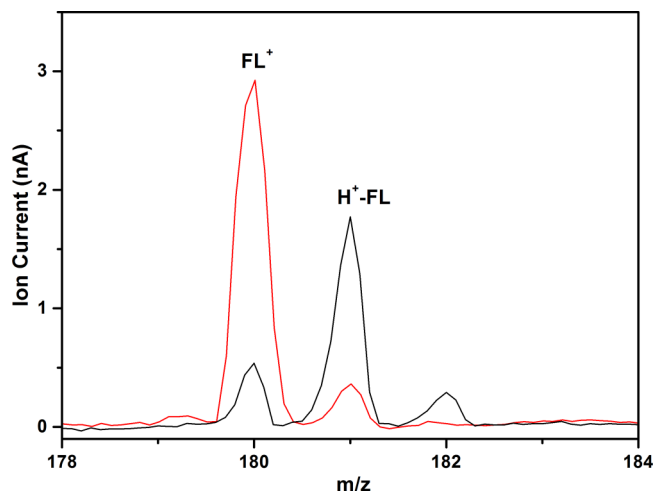

FIG. 1. Section of the mass spectrum of 9-fluorenone **FL** vapor (red) and in the presence of ethanol (black) in the hot cathode discharge source.

most stable protonation site as well as for the assignment of the carriers of the absorptions. Ground state optimization of the plausible protonated isomers of **H-FL**$^+$ and **H-DBT**$^+$ was carried out with the DFT method using a cc-pVDZ basis set and the hybrid B3LYP functional in the Gaussian 09 programme.[25] Relative ground state energies for the **H-FL**$^+$ isomers [**A**$^+$–**E**$^+$] are listed in Chart 2. Isomer **A**$^+$ with proton attached to the oxygen atom is found to be the most stable and **C**$^+$ is next, 75 kJ/mol to higher energy. A similar tendency is observed for **H-DBT**$^+$; among the six **F**$^+$–**K**$^+$ isomers **F**$^+$ obtained by protonating the oxygen atom of **DBT** is found as the global minimum. The next stable **E**$^+$ is found 105 kJ/mol higher in energy (Chart 2). Therefore, the most stable structures: **A**$^+$ and **F**$^+$, designated as **H-FL**$^+$ and H-**DBT**$^+$, were selected for excitation energy calculations.

The coordinates of **FL**$^+$, **H-FL**$^+$, **DBT**$^+$, **H-DBT**$^+$ and their neutral counterparts were optimized with the DFT method using the correlation consistent (cc-pVTZ) basis set and the M06-2X functional,[26] which is more suitable to PAHs due to inclusion of dispersive effects.[27] These coordinates were used for the calculations of vertical excitation energies. A real minimum was found for **DBT**$^+$ in C_S symmetry, which lies 2.0 kJ/mol below the C_{2V} structure. Nevertheless, the C_{2V} geometry was also used for the excitation energy calculations.

Vertical excitation energies were calculated with TD DFT, SAC-CI[28,29] implemented in Gaussian 09, and MS-CASPT2 methods;[30] the latter uses the Molcas software.[31] In the SAC-CI calculations, the cc-pVDZ basis set was used and about 200 orbitals with an energy <3 Hartree were exploited. In CASPT2 calculations state averaging was utilized; wavefunctions were optimized for the mean energy of the electronic states computed (usually 5–8 depending on symmetry of molecule). An active space was constructed from twelve electrons distributed over twelve orbitals (12,12) in the case of singlets and (11,12) for doublets with the exception of **H-DBT**$^+$ where the active space was reduced to (10,10).

IV. RESULTS AND DISCUSSION

A. 9–fluorenone cation and protonated 9–fluorenone

Spectra recorded after mass–selected deposition of the 9-fluorenone **FL**$^+$ cation with neon including a trace of CH_3Cl reveal four moderately intense absorption features in the 580-660 nm range. The strongest band is apparent at 649.2 nm and three weaker ones lying 211, 419, and 1463 cm^{-1} to higher energy (Figure 2, red trace). Thereafter, the matrix was exposed to $\lambda < 260$ nm photons which cause detachment of electrons from Cl^-. Electrons migrate in solid neon at 6 K and neutralize cations. The same rate of decrement of band intensities after
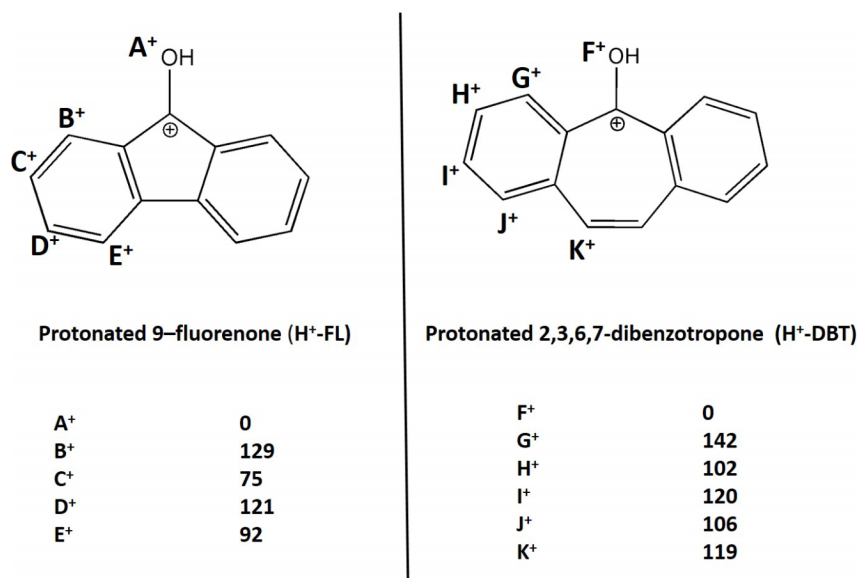
CHART 2. Structure and relative ground state energies (kJ/mol) of the **H-FL**[+] and **H-DBT**[+] isomers, calculated with DFT using the cc-pVDZ basis set and the B3LYP hybrid functional.

irradiation (black trace) indicates that all of them belong to one 649 nm system and the carrier is cationic (Table I). No new bands appeared after irradiation suggesting that neutral 9-fluorenone **FL** has absorptions beyond the detection range. The strongest transition of **FL** has been detected around 245 nm in solvents.[32,33]

FL has been previously studied by photoelectron (PE) spectroscopy.[34] The PE spectrum reveals a triplet structure at 0.86, 0.99, and 1.18 eV and a distinct band at 1.91 eV above the ground state of **FL**[+]. Vertical excitation energies of **FL**[+] were calculated (Table II) with TD DFT, SAC-CI, and MS(5)-CASPT2 (11,12) methods to assign the detected electronic absorptions in the current matrix experiment. All three methods predict low-lying electronic states $1\,^2A_2$, $1\,^2B_1$, $1\,^2B_2$ above the $\tilde{X}\,^2A_2$ ground state with energies close to the derived ones by PE study. A strong electronic transition with oscillator strength f = 0.15–0.30 to the $2\,^2B_1$ state with energy 2.10–2.35 eV agrees well with the observation at 649 nm (1.91 eV); the band 1.91 eV above the ground state of the ion seen in PE spectrum corresponds to this $2\,^2B_1 \leftarrow \tilde{X}\,^2A_2$ transition.

The TD DFT and CASPT2 calculations predict also a strong $3\,^2B_1 \leftarrow \tilde{X}\,^2A_2$ transition between 3.1 and 3.4 eV which has not been observed experimentally. TD DFT and CASPT2 likely overestimated the f values. A discussion on the theoretical methods is given in supplementary material.[38]

The three vibrational bands apparent in the spectrum are due to excitation of the ν_{21}, ν_{20}, and ν_9 totally symmetric modes in the $2\,^2B_1$ excited electronic state of **FL**[+]. The assignment

TABLE I. Absorption band maxima (±0.1 nm) of electronic transitions of 9-fluorenone cation **FL**[+] and protonated fluorenone **H**[+]**-FL** in 6 K neon matrices and assignment based on the vibrational frequencies of the normal modes listed in the footnote. Frequencies of the totally symmetric vibrations (cm^{-1}) of **FL**[+] and **H**[+]**-FL** cations calculated with DFT using the M06-2X functional and the cc-pVTZ basis set.

λ (nm)	ν (cm^{-1})	$\Delta\nu$ (cm^{-1})		Assignment
FL[+a]				
649.2	15 404	0	0_0^0	$2\,^2B_1 \leftarrow \tilde{X}\,^2A_2$
640.4	15 615	211	ν_{21}	
632.0	15 823	419	ν_{20}	
592.9	16 866	1463	ν_9	
H^{+}**-FL**[b]				
423.3	23 624	0	0_0^0	$2\,^1A' \leftarrow \tilde{X}\,^1A'$
419.2	23 855	231	ν_{43}	
416.2	24 027	403	ν_{41}	
413.8	24 166	542	ν_{39}	
409.5	24 420	796	ν_{35}	
406.7	24 588	964	ν_{33}	
404.6	24 716	1092	ν_{30}	
402.7	24 832	1208	ν_{24} or ν_{25}	
399.8	25 013	1389	ν_{20}	
393.2	25 432	1808	$\nu_{20} + \nu_{41}$	
391.4	25 549	1925	$\nu_{20} + \nu_{39}$	

^{a}**FL**[+] (C_{2v}); (a_1)ν_1–ν_{21}: 3227, 3225, 3214, 3201, 1899, 1680, 1594, 1525, 1465, 1420, 1357, 1253, 1189, 1169, 1113, 1028, 783, 720, 557, 415, 200.
^{b}**H**[+]**-FL** (C_S); (a') ν_1–ν_{43}: 3759, 3242, 3235, 3213, 3212, 3205, 3201, 3200, 3172, 1671, 1681, 1690, 1667, 1601, 1530, 1526, 1495, 1494, 1439, 1392, 1326, 1323, 1290, 1229, 1209, 1204, 1197, 1178, 1122, 1113, 1056, 1053, 1029, 921, 786, 743, 638, 623, 560, 508, 423, 275, 208.
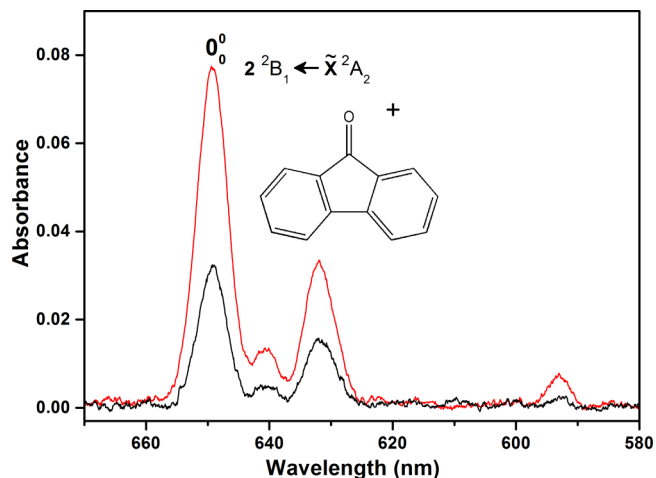

FIG. 2. Electronic absorption spectrum recorded after deposition of 9-fluorenone cation **FL**[+] into a neon matrix (red trace) and after neutralization of the cations with UV photons λ < 260 nm (black trace).

TABLE II. Electronic states, vertical excitation energies (eV) and oscillator strengths (italics) of 9-fluorenone cation and protonated 9-fluorenone calculated with TD DFT/M06-2X/cc-pVTZ, SAC-CI/cc-pVDZ, and MS(5)-CASPT2/cc-pVTZ using coordinates from DFT M06-2X/cc-pVTZ.

State	TD DFT		SAC-CI		CASPT2	
FL$^+$ C$_{2v}$						
X̃ ^{2}A$_2$	0.00		0.00		0.00	
1 ^{2}A$_2$	1.51	*0.001*	1.53	*0.001*	1.26	*0.002*
1 ^{2}B$_1$	1.68	*0.0004*	1.63	*0.002*	1.43	*0.001*
2 ^{2}B$_1$	2.09	*0.18*	2.34	*0.320*	2.14	*0.150*
3 ^{2}B$_1$	3.36[a]	*0.084*	4.73	*0.003*	3.12	*0.260*
4 ^{2}B$_1$	4.52	*0.014*	6.26	*0.120*	4.21	*0.000*
1 ^{2}B$_2$	1.65	*0.0000*	1.20	*0.000*	1.48	*0.000*
H-FL$^+$ C$_s$						
X̃ ^{1}A′	0.00		0.00		0.00	
1 ^{1}A′	2.19	*0.003*	1.54	*0.001*	2.00	*0.021*
2 ^{1}A′	3.55	*0.23*	2.93	*0.220*	3.26	*0.230*
3 ^{1}A′	4.24	*0.003*	3.75	*0.002*	3.94	*0.004*
4 ^{1}A′	4.89	*0.17*	4.54	*0.200*	4.61	*0.008*
5 ^{1}A′	5.49	*0.88*	5.14	*0.930*	4.77	*0.085*

[a]Spin contaminated state ⟨S^2⟩ = 0.9 instead 0.75. The active space in the CASPT2 calculations was (11,12) for **FL$^+$** and (12, 12) in case of **H-FL$^+$**.

given in Table I is based on the ground state frequencies calculated at the DFT/M06-2X/cc-pVTZ level.

The absorption spectrum recorded after a mass-selective deposition of protonated fluorenone cation **H-FL$^+$**, m/z = 181, shows an intense band at 423.3 nm with several weaker peaks between 390 and 420 nm (red trace, Figure 3). The double headed features separated by 20-25 cm^{-1} are evident for most of the peaks. This is due to trapping of the species at energetically non-equivalent neon sites. Thereafter, the matrix was exposed to λ < 260 nm photons. All the absorption bands diminished at the same rate on irradiation (black trace, Figure 3). This indicates that these absorptions belong to one electronic system with origin at 423.3 nm and the carrier is cationic. No new peaks appeared after irradiation.
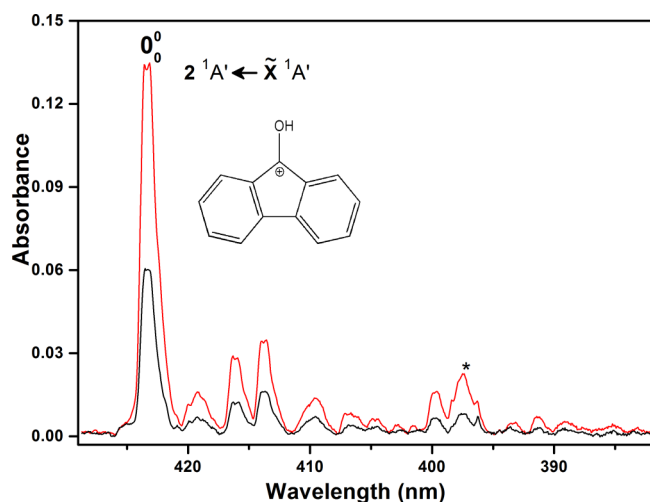
The absorptions recorded after depositing **H-FL$^+$** do not coincide with any band of **FL$^+$**. The contribution of ^{13}C isotopologue of **FL** to **H$^+$-FL** (m/z = 181) ion current was negligible with higher pressure of ethanol in the source (black trace, Figure 1).

Calculations of the ground state energies of five plausible isomers of protonated fluorenone (Chart 2) indicate that structure **A$^+$** is by far the most stable and expected to be the carrier of the 423 nm absorption system. Calculated vertical excitation energies of **A$^+$** with TDDFT, SAC-CI, and MS(6)-CASPT2(12,12) (Table II) predict a strong 2 ^{1}A′ ← X̃ ^{1}A′ electronic transition at 3.55, 2.93, and 3.26 eV, respectively, and two others with energy ~4.5 and ~5.5 eV beyond the experimental detection range. Therefore, the 423 nm (2.92 eV) system is assigned to the 2 ^{1}A′ ← X̃ ^{1}A′ transition of **A$^+$**, fluorenone protonated on the oxygen. The **FL$^+$** and **H-FL$^+$** are characterized by electronic absorption spectroscopy for the first time. **H-FL$^+$** has been studied by NMR in a strong acidic solution.[35]

The resolved vibrational structure apparent in the 423 nm system of **H-FL$^+$** is due to excitation of a number of modes in the 2 ^{1}A′ state. The assignment in Table I is based on the calculated ground state harmonic frequencies of **H-FL$^+$**.

After release of electrons into the matrix by UV irradiation, the neutral of structure **A$^+$** was not observed. The TD DFT and SAC-CI methods predict a much weaker transition for **A** compared to **A$^+$** (Table 1S.I in the supplementary material).[38] As the neutrals are formed in the matrix by electron recombination in some percentage of the cations, the detection of a transition with such a low oscillator strength is not expected. Photofragmentation of the cation could also be another reason.

B. Dibenzotropone cation and protonated dibenzotropone

Mass-selected **DBT$^+$** (m/z = 206) was deposited with neon containing a trace of CH$_3$Cl as scavenger. Two absorption systems were observed commencing at 472.2 nm and 896.4 nm

FIG. 3. Electronic absorption spectra recorded after deposition of m/z = 181 cations produced by the proton transfer reaction of EtOH$_2^+$ with 9-fluorenone in the source (red trace) and after irradiation of the matrix by λ < 260 nm photons (black trace). Asterisk marks the band of **H-FL$^+$**.
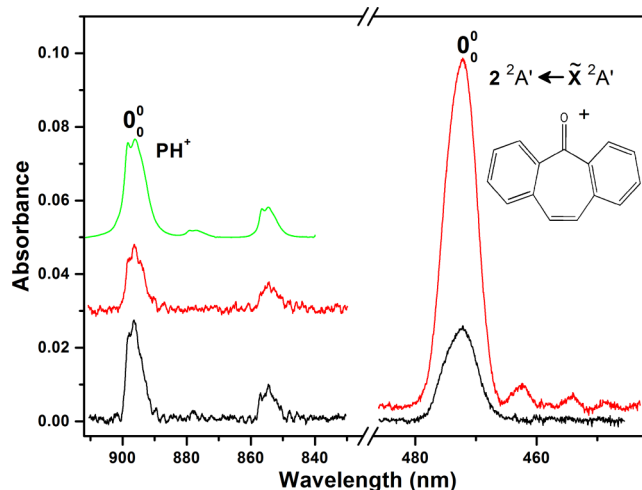

FIG. 4. Electronic absorption spectra recorded after deposition of 2,3,6,7-dibenzotropone **DBT$^+$** into a neon matrix (red trace) and after photobleaching with UV photons, λ < 260 nm (black trace). Green trace shows the spectrum obtained after deposition of phenantrane cation **PH$^+$**.

(Figure 4, red trace). The 472 nm system decreased upon UV irradiation (black trace, right section) while the 896 nm one gained in intensity (black trace, right section). Thus, the former belongs to a cation, most likely **DBT**$^+$, whereas the latter behaves in a way typical of a molecular fragment. The 896 nm absorption system is that of phenanthrene cation **PH**$^+$ (structure is shown in Chart 1);[36] the spectrum of the mass-selected **PH**$^+$ is shown in green trace of Figure 4. Thus, **DBT**$^+$ fragments to **PH**$^+$ and CO during deposition. **DBT**$^+$ is also photochemically unstable as it produced **PH**$^+$ upon UV irradiation. Release of CO from trapped ketones in a neon matrix upon UV exposure has been observed previously.[37]

    DBT has been studied by PE spectroscopy and semi-empirical calculations indicated that the ground state of **DBT**$^+$ has $^2B_1$ symmetry.[16] In the PE spectrum, a band lying at 2.64 eV above the ground state of the cation is present. This energy is close to the 472 nm (2.63 eV) system observed in a neon matrix after deposition of **DBT**$^+$. Optimization of the ground state geometry revealed that the cation as well as neutral molecule has a saddle point at C_{2v} symmetry and a real minimum at C_s. Nevertheless, the C_{2v} coordinates were used for the vertical excitation energy calculations. TD DFT, SAC-CI, and MS(5)-CASPT2 all predict a strong $2\,^2A_2 \leftarrow \tilde{X}\,^2B_1$ transition with energy 1.86–2.03 eV (f = 0.12-0.26). As no absorption was detected in the near infrared, the calculated vertical energy and/or the oscillator strength of the $2\,^2A_2 \leftarrow \tilde{X}\,^2B_1$ transition are overestimated.

    The TD DFT, CASPT2, and SAC-CI indicate a moderately intense $2\,^2B_1 \leftarrow \tilde{X}\,^2B_1$ transition with energy 3.15, 3.13, and 3.52 eV (Table III), respectively; the two former methods also give an even stronger $3\,^2A_2 \leftarrow \tilde{X}\,^2B_1$ transition at 3.26 and 2.95 eV. The $3\,^2A_2$ state of **DBT**$^+$ can only be accessed from the ground state of **DBT** via a two photon process (see Section 1 in the supplementary material),[38] therefore, the state obtained at 2.64 eV by the PE study does not correspond to $3\,^2A_2$. Hence, the band present in PE spectrum of **DBT** at 2.64 eV corresponds to the $2\,^2B_1$ state of the cation and the absorption starting at 472 nm (2.63 eV) belongs to the $2\,^2B_1 \leftarrow \tilde{X}\,^2B_1$ electronic transition of **DBT**$^+$. The CASPT2 calculations provide the best estimate of the energy of this transition, overestimate by 0.5 eV. Vertical excitation energies calculated with the coordinates optimized at C_s symmetry give similar results (Table II). As the **DBT**$^+$ is not planar, the 472 nm system is assigned to the $2\,^2A' \leftarrow \tilde{X}\,^2A'$ electronic transition (corresponding to $2\,^2B_1 \leftarrow \tilde{X}\,^2B_1$ in higher symmetry).

    The electronic spectrum of **DBT**$^+$ is simple and consists of a strong origin band at 472.2 nm and two weaker vibrational bands lying 445, 845 cm^{-1} to the blue. The assignment is based on the calculated ground state frequencies (Table IV).

    Two electronic systems starting at 502.3 and 371.5 nm were detected after mass-selected deposition of the $m/z = 207$, **H-DBT**$^+$ cations (red trace, Figure 5). Resolved vibrational structure is apparent for both electronic systems. Exposition of the matrix to $\lambda < 260$ nm photons caused a decrease in intensity for all the bands (black trace) implying cationic carrier. The rate of decrement suggests that the 502.3 and 371.5 nm absorption systems are of same **H-DBT**$^+$ isomer.

    As in the case of **H**$^+$-**FL**, protonation on the oxygen site gives the most stable isomer **F**$^+$ of **H**$^+$-**DBT** which is believed

TABLE III. Electronic states, vertical excitation energies (eV) and oscillator strengths (italics) of 2,3,6,7-dibenzotropone cation **DBT**$^+$ and protonated dibenzotropone **H-DBT**$^+$ calculated at the TD DFT/M06-2X/cc-pVTZ, SAC-CI/cc-pVDZ, and MS(5)-CASPT2/cc-pVDZ level using coordinates from DFT M06-2X/cc-pVTZ. The active space used in CASPT2 calculations was (11,11) for **DBT**$^+$ and (10,10) for **H-DBT**$^+$.

State	TD DFT		SAC-CI		CASPT2	
DBT$^+$ C_{2v}						
$\tilde{X}\,^2B_1$	0.00		0.00		0.00	
$1\,^2B_1$	1.65	*0.0013*	1.64	*0.002*	1.47	*0.001*
$2\,^2B_1$	3.15	*0.033*	3.52	0.075	3.13	*0.017*
$1\,^2A_2$	1.79	*0.0066*	1.82	0.002	1.53	*0.025*
$2\,^2A_2$	1.86	*0.13*	2.03	0.260	1.92	*0.120*
$3\,^2A_2$	3.26	*0.32*	5.13	0.000	2.95	*0.550*
$1\,^2B_2$	1.77	*0.0000*	1.62	0.000	1.48	*0.000*
DBT$^+$ C_s						
$\tilde{X}\,^2A'$	0.00		0.00		0.00	
$1\,^2A'$	1.74	*0.0017*	1.72	*0.002*	1.50	*0.002*
$2\,^2A'$	3.15	*0.038*	3.51	*0.072*	3.09	*0.013*
$3\,^2A'$	4.02	*0.0002*	4.85	*0.007*	4.12	*0.020*
$4\,^2A'$	4.30	*0.0014*	5.46	*0.001*	4.41	*0.005*
$1\,^2A''$	1.53	*0.081*	1.40	*0.005*	1.40	*0.003*
$2\,^2A''$	1.95	*0.065*	1.85	*0.034*	1.70	*0.280*
$3\,^2A''$	3.34	*0.31*	2.07	*0.220*	3.28	*0.510*
$4\,^2A''$	3.82	*0.0084*	4.76	*0.000*	4.19	*0.000*
$5\,^2A''$	3.97	*0.0038*	5.15	*0.001*	4.73	*0.003*
$6\,^2A''$	4.99	*0.0009*	5.28	*0.000*	5.04	*0.003*
H-DBT$^+$ C_1						
$\tilde{X}\,^1A$	0.00		0.00		0.00	
$1\,^1A$	3.06	*0.058*	2.23	*0.059*	3.01	*0.084*
$2\,^1A$	3.76	*0.005*	3.29	*0.032*	3.84	*0.140*
$3\,^1A$	4.28	*0.21*	3.67	*0.096*	4.41	*0.180*
$4\,^1A$	4.82	*1.13*	4.45	*1.430*	4.80	*1.170*
$5\,^1A$	4.88	*0.13*	4.57	*0.016*	5.05	*0.140*
$6\,^1A$	5.23	*0.055*	4.86	*0.047*	5.45	*0.003*

to be absorber. TD DFT and CASPT2 predict two ^1A electronic states below 4 eV, whereas SAC-CI three (Table III). The two former methods locate a moderately intense lowest energy $1\,^1A \leftarrow \tilde{X}\,^1A$ transition around 3 eV, while the latter at 2.23 eV, comparable with 502 nm (2.47 eV) system. The TD DFT and CASPT2 calculations overestimate the observed value by ~0.5 eV. The 502 nm system is assigned to the $1\,^1A \leftarrow \tilde{X}\,^1A$ transition of **H-DBT**$^+$. According to TD DFT, the transition to the $2\,^1A$ state is expected around 3.76 eV with f = 0.005, next is at 4.28 eV with f = 0.21. SAC-CI and CASPT2 give the $2\,^1A \leftarrow \tilde{X}\,^1A$ transition at 3.29 eV (f = 0.032) and 3.84 eV (f = 0.14), respectively, which can be compared with 3.34 eV (371.5 nm) in the spectrum. The assignment of the vibrational bands (Table IV) is made on the basis of calculated ground state harmonic vibrational frequencies of **H-DBT**$^+$.

    Though no new bands were detected after neutralization of the trapped cations, the expected electronic transitions of **F** were calculated (Table 1S.I in the supplementary material).[38] The TD DFT results are less reliable because the wavefunctions of the excited states are spin contaminated: $\langle S^2 \rangle$ is >0.9 instead of 0.75. SAC-CI predicts two electronic transitions at 3.63 and 4.08 eV with an intensity similar as for **H-DBT**$^+$. If

TABLE IV. Absorption band maxima (±0.1 nm) of electronic transitions of 2,3,6,7-dibenzotropone cation **DBT**$^+$ and protonated dibenzotropone **H-DBT**$^+$ in 6 K neon matrices and assignment based on the vibrational frequencies of the normal modes listed in the footnote. Frequencies of the totally symmetric vibrations (cm^{-1}) of **DBT**$^+$ and **H-DBT**$^+$ calculated with DFT using the M06-2X functional and the cc-pVTZ basis set.

λ (nm)	ν (cm^{-1})	$\Delta\nu$ (cm^{-1})		Assignment
DBT^{+a}				
472.2	21 177	0	0_0^0	$2\,^2A' \leftarrow \tilde{X}\,^2A'$
462.5	21 622	445	ν_{31}	
454.1	22 022	845	ν_{23} or ν_{24}	
H-DBT^{+b}				
502.4	19 904	0	0_0^0	$1\,^1A \leftarrow \tilde{X}\,^1A$
493.3	20 272	368	ν_{67}	
474.3	21 084	1180	ν_{33} or ν_{34}	
470.3	21 263	1359	ν_{25}	
466.0	21 459	1555	ν_{16} or ν_{17}	
371.5	26 918	0	0_0^0	$2\,^1A \leftarrow \tilde{X}\,^1A$
358.1	27 925	1007	ν_{43}	
353.6	28 281	1363	ν_{25}	

^{a}**DBT**$^+$ (C_S); $\nu_1 - \nu_{37}$: 3237, 3224, 3214, 3212, 3200, 1791, 1660, 1621, 1592, 1533, 1468, 1406, 1352, 1273, 1206, 1195, 1190, 1124, 1076, 1059, 1029, 953, 887, 838, 819, 792, 682, 674, 589, 511, 468, 400, 318, 253, 209, 125, 44.
^{b}**H-DBT**$^+$ (C_1); $\nu_1 - \nu_{75}$: 3810, 3248, 3228, 3218, 3218, 3211, 3208, 3203, 3199, 3193, 3189, 1700, 1679, 1674, 1614, 1598, 1548, 1533, 1529, 1495, 1480, 1447, 1437, 1407, 1392, 1318, 1230, 1282, 1264, 1235, 1219, 1215, 1207, 1191, 1169, 1141, 1095, 1082, 1062, 1056, 1048, 1030, 1016, 941, 936, 920, 877, 862, 841, 832, 799, 782, 757, 735, 697, 687, 625, 604, 587, 579, 555, 516, 497, 478, 422, 413, 384, 331, 324, 270, 218, 195, 138, 80, 50.
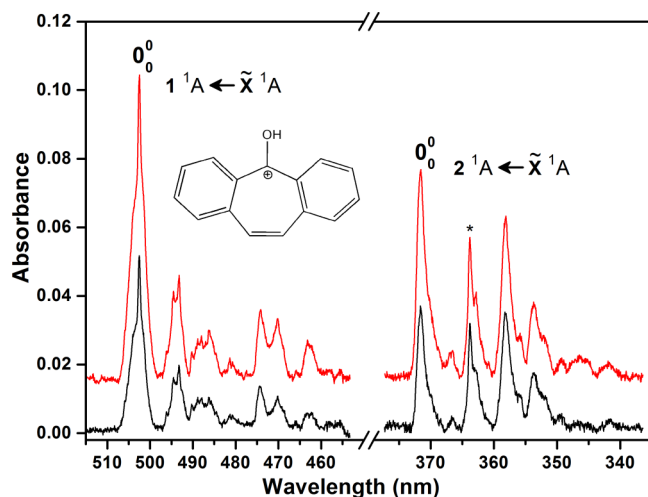

FIG. 5. Electronic absorption spectra recorded after depositing m/z = 207 cations produced by protonation of 2,3,6,7-dibenzotropone in the source using ethanol (red trace), and after irradiation of the matrix by $\lambda < 260$ nm photons (black trace).

the oscillator strengths are correct the neutral should also be detected, in contrast to the observation. Protofragmentation of the cations could be the reason for the lack of detection of **F**.

V. CONCLUDING REMARKS

The studied O-PAH class of molecules is astrobiologically interesting as they have been found in lipids, vitamins, pigment, and are involved in electron transport. Aromatic ketones are also present in plants, fungi, lichens. Identification

of 9-fluorenone in Murchison meteorite suggests that such aromatic ketones can be present on cosmic ices; ice photolysis in astronomical environments is believed to be the leading chemical process for the formation of the oxidized PAHs. They may also be found in the gas phase because complex organics detected in the interstellar medium are thought to be formed in cold grain surfaces and thereafter delivered into gas phase through ablation by shock waves or heating from stars/supernova. Spectroscopic knowledge is required for the *in situ* detection of such molecules and this work provides the data on the protonated O-PAHs systems in inert neon matrices at 6 K and is a starting point for gas phase studies.

[1]L. J. Allamandola, D. J. Hudgins, and S. A. Sandford, Astrophys. J. **511**, L115 (1999).
[2]L. J. Allamandola, S. A. Sandford, and B. Wopenka, Science **237**, 56 (1987).
[3]M. K. Crawford, A. G. G. M. Tielens, and L. J. Allamandola, Astrophys. J. **293**, L45 (1985).
[4]T. Onaka, I. Yamamura, T. Tanabe, T. L. Roellig, and L. Yuen, Publ. Astron. Soc. Jpn. **48**, L59 (1996).
[5]J. Kahanpää, K. Mattila, K. Lehtinen, C. Leinert, and D. Lemke, Astron. Astrophys. **405**, 999 (2003).
[6]I. Sakon, T. Onaka, D. Ishihara, T. Ootsubo, I. Yamamura, T. Tanabé, and T. L. Roellig, Astrophys. J. **609**, 203 (2004).
[7]M. P. Bernstein, J. E. Elsila, J. P. Dworkin, S. A. Sandford, L. J. Allamandola, and R. N. Zare, Astrophys. J. **576**, 1115 (2002).
[8]S. F. M. Ashbourn, J. E. Elsila, J. P. Dworkin, M. P. Bernstein, S. A. Sandford, and L. J. Allamandola, Meteorit. Planet. Sci. **42**, 2035 (2007).
[9]E. E. Hardegree-Ullman, M. S. Gudipati, A. C. A. Boogert, H. Lignell, L. J. Allamandola, K. R. Stapelfeldt, and M. Werner, Astrophys. J. **784**, 172 (2014).
[10]M. P. Bernstein, S. A. Sandford, L. J. Allamandola, J. S. Gillette, S. J. Clemett, and R. N. Zare, Science **283**, 1135 (1999).
[11]M. P. Bernstein, S. A. Sandford, A. L. Mattioda, and L. J. Allamandola, Astrophys. J. **664**, 1264 (2007).
[12]J. Bouwman, H. M. Cuppen, A. Bakker, L. J. Allamandola, and H. Linnartz, Astron. Astrophys. **511**, A33 (2010).
[13]P. J. Sarre, J. Mol. Spectrosc. **238**, 1 (2006).
[14]F.-X. Hardy, O. Gause, C. A. Rice, and J. P. Maier, Astrophys. J. **778**, L30 (2013).
[15]C. A. Rice, F.-X. Hardy, O. Gause, and J. P. Maier, J. Phys. Chem. Lett. **5**, 942 (2014).
[16]M. Allan, E. Heilbronner, and E. Kloster-Jensen, J. Electron Spectrosc. Relat. Phenom. **6**, 181 (1975).
[17]B. P. Balise, B. S. Middleditch, and J. Oro, Org. Geochem. **5**, 211 (1984).
[18]R. V. Krishnamurthy, J. R. Cronin, S. Pizzarello, and G. U. Yuen, Geochim. Cosmochim. Acta **56**, 4045 (1992).
[19]G. D. Cody and C. M. Alexander, Geochim. Cosmochim. Acta **69**, 1085 (2005).
[20]A. L. Knecht, B. C. Goodale, L. Truong, M. T. Simonich, A. J. Swanson, M. M. Matzke, K. A. Anderson, K. M. Waters, and R. L. Tanguay, Toxicol. Appl. Pharmacol. **271**, 266 (2013).
[21]J. Konig, E. Balfanz, W. Funcke, and T. Romanowsk, Anal. Chem. **55**, 599 (1983).
[22]E. M. Fitzpatrick, A. B. Ross, J. Bates, G. Andrews, J. M. Jones, H. Phylaktou, M. Pourkashanian, and A. Williams, Process Saf. Environ. Prot. **85**, 430 (2007).
[23]I. Garkusha, J. Fulara, P. J. Sarre, and J. P. Maier, J. Phys. Chem. A **115**, 10972 (2011).
[24]R. Rossetti and L. E. Brus, Rev. Sci. Instrum. **51**, 467 (1980).

[25]M. J. Frisch, G. W. Trucks, H. B. Schlegel, G. E. Scuseria, M. A. Robb, J. R. Cheeseman, G. Scalmani, V. Barone, B. Mennucci, G. Petersson *et al.*, GAUSSIAN 09, Revision D.01, Gaussian Inc., Wallingford, CT, 2009.

[26]Y. Zhao and D. G. Truhlar, Theor. Chem. Acc. **120**, 215 (2008).

[27]A. Y. Rogachev, A. S. Filatov, A. V. Zabula, and M. A. Petrukhina, Phys. Chem. Chem. Phys. **14**, 3554 (2012).

[28]H. Nakatsuji and K. Hirao, J. Chem. Phys. **68**, 2053 (1978).

[29]H. Nakatsuji, Chem. Phys. Lett. **67**, 329 (1979).

[30]J. Finley, P.-Å Malmqvist, B. O. Roos, and L. Serrano-Andrés, Chem. Phys. Lett. **288**, 299 (1998).

[31]F. Aquilante, L. De Vico, N. Ferré, G. Ghigo, P.-Å Malmqvist, P. Neogrády, T. B. Pedersen, M. Pitonak, M. Reiher, B. O. Roos, L. Serrano-Andrés, M. Urban, V. Veryazov, and R. Lindh, J. Comput. Chem. **31**, 224 (2010).

[32]A. I. Adeogun, N. W. Odozi, N. O. Obiegbedi, and O. S. Bello, Afr. J. Biotechnol. **7**, 2736 (2008).

[33]K. K. Ding and C. P. Pan, Crystallogr. Rep. **58**, 604 (2013).

[34]G. Centineo, I. Fragala, G. Bruno, and S. Spampinato, J. Mol. Struct. **44**, 203 (1978).

[35]G. A. Olah, G. K. Surya prakash, G. Liang, P. W. Westerman, K. Kunde, J. Chandrasekhar, and P. V. R. Schleyer, J. Am. Chem. Soc. **102**, 4485 (1980).

[36]A. Chakraborty, J. Fulara, and J. P. Maier, J. Phys. Chem. A **109**, 50 (2015).

[37]F. Salama, C. Joblin, and L. J. Allamandola, J. Chem. Phys. **101**, 10252 (1994).

[38]See supplementary material at http://dx.doi.org/10.1063/1.4929484 for the HOMO and LUMO energies of DBT and DBT$^+$ (Figure 1S.I, Figure 1S.II), discussion on computational discrepancy (Section 1S), optimized coordinates used for excitation energy calculations (Chart 1S), and calculated vertical excitation energies of H-FL and H-DBT (Table 1S.I).